Part I

AGNs, starbursts and galaxy evolution

1

The effects of mass and star-formation timescale on galaxy evolution

Craig D. Harrison & Matthew Colless

1.1 Introduction

In a ΛCDM cosmology, the growth of structure occurs hierarchically; small objects form first and undergo mergers to form more massive objects. Modelling the formation and evolution of galaxies with numerical simulations is impossible because crucial aspects lack a complete physical model – notably, feedback and star formation.

An alternative to full numerical simulations is the semi-analytic models (Croton *et al.* 2006; De Lucia *et al.* 2006), so called because they use approximate prescriptions for physical processes that are poorly understood. These prescriptions contain parameters that are set by demanding that the model reproduces the observations of (typically) low-redshift galaxies. The process itself is often motivated by a result from a more detailed numerical simulation or from observations.

The cooling of gas is central to the process of galaxy formation, as it sets the rate at which gas becomes available for star formation. Feedback processes have the largest impact on the predictions for galaxy properties, as these processes affect the efficiency of galaxy formation by increasing the cooling time of hot gas and suppressing further star formation. Previous iterations of the semi-analytic models (Kauffmann 1996), which lacked a prescription for feedback, predicted that the galaxy population should continue to evolve at $z < 1$, at a rate greater than that due to passive evolution, as more massive galaxies are built up by continued mergers. These mergers of galaxies with gas reserves (wet mergers) are accompanied by a burst of star formation and, consequently, massive galaxies are predicted to exhibit younger ages and higher metallicities than less massive galaxies. More recent models incorporating 'radio mode' feedback from AGN, which suppresses star formation in massive galaxies at higher redshifts (Croton *et al.* 2006), predict that while early-type galaxies assemble their mass hierarchically they have

AGN Feedback in Galaxy Formation, eds. V. Antonuccio-Delogu and J. Silk. Published by Cambridge University Press.

anti-hierarchical star-formation histories (De Lucia *et al.* 2006). In these models, massive early-type galaxies are predicted to be older, more metal-rich, and have higher α-element abundance ratios than less massive galaxies, even though their mass assembly was completed at a later time through purely stellar mergers (dry mergers). Trends of decreasing mass, age and metallicity with increasing cluster-centric distance are also predicted.

We test the predictions from these more recent models by analysing the stellar populations of cluster early-type galaxies. Redshifts, velocity dispersions and Lick absorption-line strengths (Burstein *et al.* 1984; Trager *et al.* 1998) are measured for $\sim$100 galaxies from four clusters. The ages, metallicities and α-element abundance ratios of these galaxies are estimated by comparison of the absorption-line strengths with up-to-date stellar population models.

1.2 Estimating the stellar population parameters

The stellar population parameters, age (t), metallicity ($[Z/\mathrm{H}]$) and α-element abundance ratio ($[\alpha/\mathrm{Fe}]$), were estimated for $\sim$100 galaxies in four low-z clusters. These clusters have $\langle z \rangle = 0.04$ and were selected to span the range of both Abell richness classes and B-M classifications.

Along with the redshift (z) and velocity dispersion (σ), the strengths of three Lick absorption-line indices, Hβ, Mg b, and Fe5335, were measured for each galaxy. These strengths were then corrected for σ broadening before being calibrated to the Lick system.

The stellar population parameters were estimated using a method similar to Proctor *et al.* (2004) and compared to the predictions from the Thomas *et al.* (2003) single stellar population models. The models were interpolated in steps of 0.25 Gyr in t and 0.025 dex in $[Z/\mathrm{H}]$ and $[\alpha/\mathrm{Fe}]$.

The ratio of α-elements to Fe is commonly interpreted as a measure of star-formation timescale. Fe is predominantly created in SNIa while α-elements are predominantly created in SNII. Since there is a delay between the onset of SNII and SNIa, $[\alpha/\mathrm{Fe}]$ can be used as a chronometer to estimate the duration of star formation.

1.3 Scaling relations

Figure 1.1 shows the variations of t (left), $[Z/\mathrm{H}]$ (middle), and $[\alpha/\mathrm{Fe}]$ (right) with σ. Mean error bars are shown in the bottom right corner of each panel. The solid lines in each panel are the linear fits to the data (the dashed lines in the left panel are visual aids that will be discussed later). A significant correlation with σ is found for both $[Z/\mathrm{H}]$ and $[\alpha/\mathrm{Fe}]$. Performing linear fits to the relations, taking into account

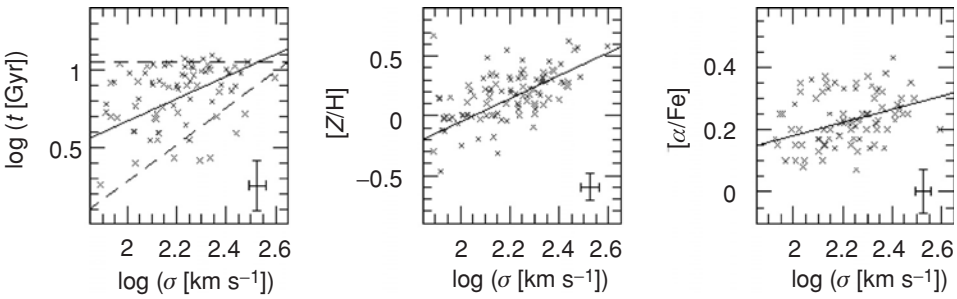

Figure 1.1 The variation of the stellar population parameters with σ. The solid line in each panel is the fit to the data. The dashed lines are simply guides for the eyes.

the errors in both quantities, we find

$$\log(t) = (0.72 \pm 0.09)\ \log\sigma - (0.77 \pm 0.21),$$
$$[Z/\mathrm{H}] = (0.97 \pm 0.08)\ \log\sigma - (1.99 \pm 0.17),$$
$$[\alpha/\mathrm{Fe}] = (0.21 \pm 0.05)\ \log\sigma - (0.24 \pm 0.12).$$

Looking at $[Z/\mathrm{H}]$ first, we find that it is strongly correlated with σ ($r_S = 0.56$), at a significance level $>5\sigma$. A moderate correlation is found between $[\alpha/\mathrm{Fe}]$ and σ ($r_S = 0.32$), a result that is significant at the 3σ level.

Given the size of the mean errors, the tightness of these two relations is remarkable, and implies that σ is a major factor in determining the $[Z/\mathrm{H}]$ and $[\alpha/\mathrm{Fe}]$ of a galaxy, with more massive galaxies being older and more metal-rich than less massive galaxies.

A moderate correlation is detected between t and σ ($r_S = 0.31$), significant at only the 2.8σ level. The distribution of points, however, is rather interesting. At all σ there exist galaxies with very old ages (marked by the horizontal dashed line), but the age of the youngest galaxy (at a given σ) increases with σ (approximately as the sloped, dashed line). This behaviour is reminiscent of down-sizing (Cowie *et al.* 1996), where the typical mass of a star-forming galaxy increases with z.

The possibility that a real correlation between t and σ exists cannot be discounted. The age limit of the models causes the build-up of galaxies on the upper edge of the distribution that may blur out any correlation and result in the conclusion of down-sizing. If this were the case, there would be an increase in the density of points on the upper edge of the distribution with increasing σ, which we do not see.

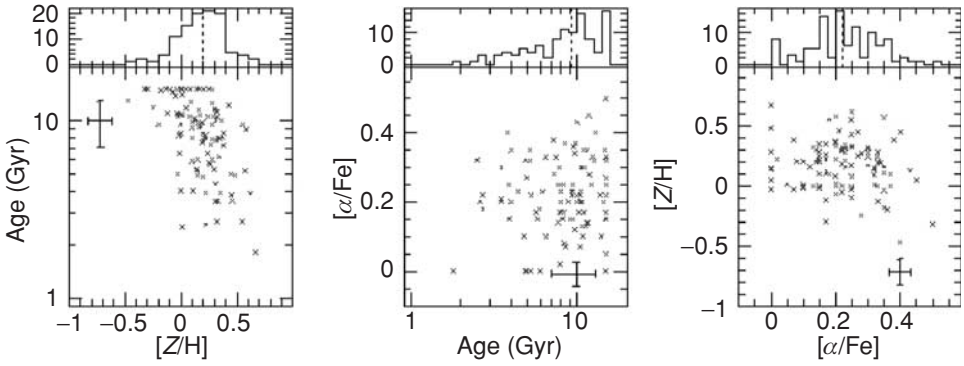

Figure 1.2 The stellar population parameter distributions and mean errors. Marginal distributions are given at the top of each panel with the median value marked with dotted lines.

Calculating ranges of the stellar population parameters predicted by these fits for a realistic range of σ, we find that they are in good agreement with the range of values observed for early-type galaxies in clusters (Trager *et al.* 2000).

These results confirm the predictions from De Lucia *et al.* (2006) that $[Z/\mathrm{H}]$ and $[\alpha/\mathrm{Fe}]$ are both positively correlated with mass. While we cannot confirm a correlation between t and mass, we do find evidence for down-sizing.

1.4 Parameter distributions

The distributions of stellar population parameters are shown in Figure 1.2. Marginal distributions are plotted for each of the parameters and the median values are marked as dotted lines. Median errors are given in each panel.

Looking at the distributions, we note that very few galaxies have $[Z/\mathrm{H}]$ less than solar with most having $0.0 \lesssim [Z/\mathrm{H}] \lesssim 0.5$ dex. Similarly, $[\alpha/\mathrm{Fe}]$ is mostly greater than solar and lies in the range $0.1 \lesssim [\alpha/\mathrm{Fe}] \lesssim 0.4$ dex. The bulk of the galaxies have old ages and almost all lie in the range $4 \lesssim t \lesssim 15$ Gyr. These distributions are in general agreement with those found by previous authors (Thomas *et al.* 2005; Collobert *et al.* 2006). The median $[Z/\mathrm{H}]$ of our sample is 0.19 ± 0.02 dex, the median t is 9.2 ± 0.5 Gyr, and the median $[\alpha/\mathrm{Fe}]$ is 0.22 ± 0.01 dex. The errors on these median values were determined from Monte Carlo simulations.

Looking at the marginal distributions, the $[Z/\mathrm{H}]$ and $[\alpha/\mathrm{Fe}]$ distributions are approximately Gaussian in nature. However, the t distribution is approximately exponential; most galaxies are old ($t \geq 8$ Gyr) but there is a tail of galaxies extending to ages as young as $\sim$2 Gyr.

It is also evident that there appears to be an anti-correlation between $[Z/\mathrm{H}]$ and t, in the sense that younger galaxies are more metal-rich. This might in principle be due to the non-orthogonal nature of the metallicity–age grids produced by the stellar population models, which means that the errors on these two quantities are correlated.

1.5 The influence of mass

The spread in the stellar population parameter distributions found for the low-z cluster sample is partly due to a combination of observational errors and the correlations with σ. To determine the amount of intrinsic scatter in the distributions, over and above that caused by the observational errors, we ran a series of numerical simulations. The method used was as follows.

Recalling that the t distribution is approximately exponential and that both the $[Z/\mathrm{H}]$ and $[\alpha/\mathrm{Fe}]$ distributions are approximately Gaussian, we began by selecting a range of e-foldings for the exponential t distribution (τ) and a range of Gaussian scatters in $[Z/\mathrm{H}]$ and $[\alpha/\mathrm{Fe}]$ ($\sigma_{[Z/\mathrm{H}]}$ and $\sigma_{[\alpha/\mathrm{Fe}]}$). The medians of the $[Z/\mathrm{H}]$ and $[\alpha/\mathrm{Fe}]$ distributions were used as the means of their Gaussian distributions, and the exponential t distribution was truncated at 5 Gyr (at younger ages the models are less reliable) and at 14 Gyr (the age of the universe).

A model was generated for each combination of τ, $\sigma_{[Z/\mathrm{H}]}$, and $\sigma_{[\alpha/\mathrm{Fe}]}$ consisting of 10 000 mock galaxies with t, $[Z/\mathrm{H}]$ and $[\alpha/\mathrm{Fe}]$ (parameter triples) drawn randomly from the specified distributions.

These parameter triples were converted to the corresponding Hβ, Mg b and Fe5335 index values (index triples). These index triples were then perturbed by randomly drawing errors from the observed galaxies' index error distributions. The perturbed index triples were converted back to parameter triples by exactly the same method used to estimate the stellar population parameters for the observed galaxies.

To ascertain how well the models fit the data a likelihood statistic was used. The stellar population parameter space was divided up into bins and the probability of each bin containing a galaxy was calculated. The t bins were 0.5 Gyr in width and ranged from 0 and 15 Gyr, the $[Z/\mathrm{H}]$ bins were 0.125 dex in width and ranged from -2.2875 to 0.7125 dex, and the $[\alpha/\mathrm{Fe}]$ bins were 0.025 dex in width and ranged from 0.0 to 0.5 dex. Monte Carlo simulations were used to estimate the probability of obtaining a likelihood statistic larger than the observed one by chance.

These simulations provide us with a great deal of information regarding the intrinsic scatter in each of the stellar population parameters. Firstly, it is difficult to constrain the e-folding of the exponential t distribution. This is due to small uncertainties in index strengths translating to large changes in the t estimate

combined with relatively large observational errors in the Hβ index. Although models with small values of e-folding are not ruled out, we find that our data are most consistent with the model having $\tau = 900$ Myr. Secondly, small scatters in $[Z/\mathrm{H}]$ ($\sigma_{[Z/\mathrm{H}]} < 0.1$ dex) are strongly ruled out, as are large scatters ($\sigma_{[Z/\mathrm{H}]} > 2.0$ dex). We find the model with $\sigma_{[Z/\mathrm{H}]} = 0.3$ dex is the most consistent with our data. Finally, large scatters in $[\alpha/\mathrm{Fe}]$ ($\sigma_{[\alpha/\mathrm{Fe}]} > 0.3$ dex) are also strongly ruled out. Models with low scatters in the $[\alpha/\mathrm{Fe}]$ are not ruled out, but we find that the most consistent model is that with $\sigma_{[\alpha/\mathrm{Fe}]} = 0.07$ dex.

As we showed above, both $[Z/\mathrm{H}]$ and $[\alpha/\mathrm{Fe}]$ are significantly correlated with σ. Since the galaxies in the low-z cluster sample have a range of σ, it is understandable that we should detect an intrinsic scatter in $[Z/\mathrm{H}]$ and $[\alpha/\mathrm{Fe}]$. The degree to which the intrinsic scatter in these parameter distributions is attributable to trends with σ can be estimated by comparing the scatter expected given the σ distribution in the cluster and the intrinsic scatter about the parameter$-\sigma$ relations. Since the correlation between t and σ is only marginal we will concentrate on the scatter in $[Z/\mathrm{H}]$ and $[\alpha/\mathrm{Fe}]$.

We use the parameter$-\sigma$ relations to convert the galaxies' σ into parameter values. The scatter in these values is then calculated; the intrinsic scatter about the relation is then added in quadrature to the scatter due to the relation with σ, and the result is compared to that obtained from the simulations described above.

The scatter expected in $[Z/\mathrm{H}]$ on this basis is 0.21 dex, which is comparable to the intrinsic scatter of $\sigma_{[Z/\mathrm{H}]} \sim 0.3$ dex estimated above. The expected scatter in $[\alpha/\mathrm{Fe}]$ is 0.06 dex, which is very close to the estimated intrinsic scatter $\sigma_{[\alpha/\mathrm{Fe}]} \sim 0.07$ dex. It appears then that the intrinsic scatter in both the $[Z/\mathrm{H}]$ and $[\alpha/\mathrm{Fe}]$ distributions can be accounted for by the parameter$-\sigma$ relation and the intrinsic scatter about it.

Which of these two sources contributes most to the scatters is an interesting question. For the $[Z/\mathrm{H}]$ distribution, we find that the major contribution comes from the correlation with σ. For the $[\alpha/\mathrm{Fe}]$ distribution, the major contribution comes from the intrinsic scatter about the $[\alpha/\mathrm{Fe}]$–σ relation. In analysing the stellar population parameter distributions in each of the four clusters, we found evidence of differences in the $[\alpha/\mathrm{Fe}]$ distributions. Thus, we attribute the intrinsic scatter about the $[\alpha/\mathrm{Fe}]$–σ relation to differences in cluster properties (e.g. its dynamical state). No variation in the $[Z/\mathrm{H}]$ distributions between clusters was found, and so we attribute the scatter in the $[Z/\mathrm{H}]$–σ relation to differences in galaxy properties.

1.6 Star formation inside out

One would expect that the projected radial distance of a galaxy from the cluster centre (R_{proj}) would be correlated with the local density: the cluster core being more

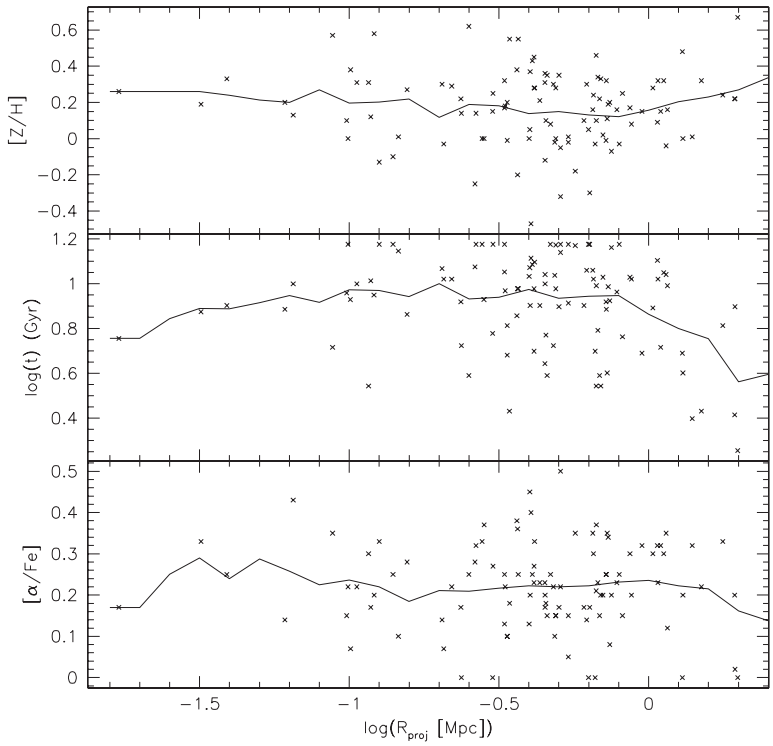

Figure 1.3 The trend of mean $[Z/\mathrm{H}]$ (*top*), mean age (*middle*), and mean $[\alpha/\mathrm{Fe}]$ (*bottom*) with projected cluster-centric radius. The mean is calculated in 0.4 dex wide bins at steps of 0.1 dex.

dense than the cluster outskirts, which in turn are more dense than the surrounding structures. Examining the stellar population parameters as functions of R_{proj} should therefore indicate variations with local density. Figure 1.3 shows the variations of each stellar population parameter with R_{proj}. The lines in these plots show the mean values in logarithmic distance bins 0.4 dex in width at 0.1 dex steps. Only galaxies inside the Abell radius (R_{Abell}) are shown, since outside this radius the galaxies are too sparsely sampled. From this figure we see that both $[Z/\mathrm{H}]$ (top) and $[\alpha/\mathrm{Fe}]$ (bottom) are essentially constant within R_{Abell}. On the other hand, t begins to decrease outside a radius of ~ 0.8 Mpc. Inside this radius $\langle t \rangle \approx 8$ Gyr, but this decreases to $\langle t \rangle \approx 4$ Gyr at R_{Abell}. This decrease is significant at the $> 4\sigma$ level. This result shows that galaxies outside the cores of clusters are more commonly younger or have had a more recent bout of star formation. These could possibly represent galaxies that have had a burst of star formation triggered by their movement into the cluster environment. These results confirm the De Lucia *et al.* (2006) prediction of t gradients within clusters. We cannot, however, confirm the predicted $[Z/\mathrm{H}]$ and $[\alpha/\mathrm{Fe}]$ radial gradients. It must be noted that the semi-analytical models have

the benefit of knowing precisely the 3D galaxy distribution, while we must use $R_{\rm proj}$. It is possible that the trends with $[Z/{\rm H}]$ and $[\alpha/{\rm Fe}]$ are blurred out because of this.

1.7 Summary

In summmary, early-type galaxies form a class of objects whose properties are largely (but not solely) determined by their mass, and which are subsequently partially modified by wet mergers that are increasingly important for lower mass galaxies. We find that $[Z/{\rm H}]$ and $[\alpha/{\rm Fe}]$ are correlated with σ, confirming the predictions from recent semi-analytic models. This implies that more massive galaxies are more metal-rich and form their stars on shorter timescales than less massive galaxies. The distribution of t (as a function of σ) is found to be consistent with down-sizing.

No trends with projected cluster-centric distance are found for $[Z/{\rm H}]$ and $[\alpha/{\rm Fe}]$, but younger galaxies are preferentially found outside the cluster core, again in agreement with the models. We conclude that 'radio mode' feedback from AGN is an important element in creating models that are consistent with observations.

References

Burstein, D., *et al.* (1984). *Astrophys. J.*, **287**, 586
Collobert, M., *et al.* (2006). *Mon. Not. R. Astron. Soc.*, **370**, 1213
Cowie, L. L., *et al.* (1996). *Astrophys. J.*, **112**, 839
Croton, D. J., *et al.* (2006). *Mon. Not. R. Astron. Soc.*, **365**, 11
De Lucia, G., *et al.* (2006). *Mon. Not. R. Astron. Soc.*, **366**, 499
Kauffmann, G. (1996). *Mon. Not. R. Astron. Soc.*, **281**, 487
Proctor, R. N., Forbes, D. A., & Beasley, M. A. (2004). *Mon. Not. R. Astron. Soc.*, **355**, 1327
Thomas, D., Maraston, C., & Bender, R. (2003). *Mon. Not. R. Astron. Soc.*, **339**, 897
Thomas, D., *et al.* (2005). *Astrophys. J.*, **621**, 673
Trager, S. C., *et al.* (1998). *Astrophys. J. Suppl.*, **116**, 1
Trager, S. C., *et al.* (2000). *Astrophys. J.*, **120**, 165

2

Suppressing cluster cooling flows by multiple AGN activity

Adi Nusser

2.1 Introduction

Models invoking only the central AGN to resolve the cooling flow conundrum in galaxy clusters require fine-tuning of highly uncertain microscopic transport properties to distribute the thermal energy over the entire cluster cooling core. A model in which the ICM is heated instead by multiple, spatially distributed AGNs bypasses most of these difficulties (Nusser *et al*. 2006). The central regions of galaxy clusters are rich in spheroidal systems, all of which are thought to host black holes and could participate in the heating of the ICM via AGN activity of varying strengths. And they do. There is mounting observational evidence for multiple AGNs in cluster environments. Active AGNs drive bubbles into the ICM. We identify three distinct interactions between the bubble and the ICM: (1) Upon injection, the bubbles expand rapidly *in situ* to reach pressure equilibrium with their surroundings, generating shocks and waves whose dissipation is the principal source of ICM heating. (2) Once inflated, the bubbles rise buoyantly at a rate determined by balance with the viscous drag force, which itself results in some additional heating. (3) Rising bubbles expand and compress their surroundings. This process is adiabatic and does not contribute to any additional heating; rather, the increased ICM density due to compression enhances cooling. Our model sidesteps the "transport" issue by relying on the spatially distributed galaxies to heat the cluster core. We include self-regulation in our model by linking AGN activity in a galaxy to cooling characteristics of the surrounding ICM. We use a spherically symmetric one-dimensional hydrodynamical code to carry out a preliminary study illustrating the efficacy of the model. Our self-regulating scenario predicts that there should be enhanced AGN activity of galaxies inside the cooling regions compared to galaxies

AGN Feedback in Galaxy Formation, eds. V. Antonuccio-Delogu and J. Silk. Published by Cambridge University Press.